

Adsorption and diffusion of hydrogen on Pd(211) and Pd(111): Results from first-principles electronic structure calculations

Sampyo Hong and Talat S. Rahman*

Department of Physics, University of Central Florida, Orlando, Florida 32816-2385, USA

(Received 4 January 2007; published 6 April 2007)

We have carried out first-principles calculations of H adsorption on Pd(211) using density-functional theory with the generalized gradient approximation in the plane-wave basis to find out that the most preferred is the threefold hollow site on the terrace of Pd(211) with an adsorption energy of 0.52 eV: the hcp and fcc sites being almost energetically equally favorable. For subsurface H adsorption on Pd(211), the octahedral site with an adsorption energy of 0.19 eV is slightly more favorable than the tetrahedral site (0.18 eV). Our calculated activation energy barrier for H to diffuse from the preferred surface site to the subsurface one on Pd(211) is 0.33 eV, as compared with 0.41 eV on Pd(111). Thus, there is an enhancement of the probability of finding subsurface hydrogen in Pd(211). Additionally, we find the diffusion barriers for H on the terraces of Pd(211) to be 0.11 eV, while that along the step edge to be only 0.05 eV and that within the second layer (subsurface) to be 0.15 eV.

DOI: [10.1103/PhysRevB.75.155405](https://doi.org/10.1103/PhysRevB.75.155405)

PACS number(s): 71.15.Mb, 82.45.Jn, 82.56.Lz, 34.50.Dy

I. INTRODUCTION

Palladium is an important material in hydrogenation catalysis, electrolysis, and hydrogen storage technology. Bulk Pd readily absorbs hydrogen through the densely packed (111) planes^{1,2} and forms a metal hydride. Hydrogen also adsorbs dissociatively on the low-index Pd surfaces, generally on the highly coordinated sites.³ For example, the most preferred adsorption of hydrogen on these surfaces appears to be on the hollow sites, for which experiments point to an adsorption energy in the range of 0.45–0.53 eV.¹ However, this argument about coordination does not hold on a stepped surface like Pd(210), for which the local variations of the electronic structure at the adsorption sites appear to also play a role.⁴ On Pd(111), experiments also suggest hydrogen occupation of a subsurface site (in the region between the first and second Pd layers) at temperatures surprisingly low as 80 K.^{5–9} These and related studies are part of the abundant literature on hydrogen adsorption on palladium surfaces. However, several issues still linger. In particular, the question of subsurface adsorption remains debatable and even more puzzling is the fact that subsurface adsorption takes place at very low temperatures. Earlier theoretical studies found subsurface site occupation to be critical to the formation of an ordered phase on the surface and subsurface occupation to be energetically favorable as the on-surface one.^{10–12} To understand the microscopic implications of subsurface versus on-surface adsorption, theoretical calculations based on first-principles density-functional theory^{13–18} (DFT) have also been carried out. The conclusion from the latter studies is that on-surface H adsorption is energetically favored, suggesting hydrogen equilibration on the surface before diffusion into the layers below the surface. At the same time, to explain the observed low-temperature subsurface H adsorption, a concerted diffusion model involving two H atoms was proposed.¹⁸ In another effort, surface phonon mediated subsurface adsorption was also suggested.¹⁶

Interesting as these results are, the debate focused mainly on the low Miller index surfaces of Pd. Since steps and other

defects are generally present on surfaces, their role in determining the energetics and dynamics of H on these surfaces needs to be understood. In this regard, the recent experimental and theoretical studies⁴ of H on Pd(210) are interesting. These authors find that H adsorption has considerable impact on the relaxation pattern of Pd(210). Additionally, local coordination alone does not explain the preference for an adsorption site for H on Pd(210). In this work, we have undertaken a comparative study of H adsorption on Pd(211), a regular stepped vicinal surface of Pd(111), and Pd(111) itself, with the intention of understanding the effect of local environment and coordination. This choice of surface geometry also allows us to further compare our results with those already outlined for Pd(210), which being a vicinal of Pd(100) is an open surface with a high density of steps. It consists of two-atom-wide (100) terraces, separated by (110)-faceted steps, while Pd(211) consists of three-atom-wide (111) terraces, separated by (100)-faceted steps.

Apart from questions about the most preferred adsorption site and the dependence of the adsorption energy on the local environment, the issue of the diffusion energy barrier for H on Pd surfaces (and subsurface) is also of technological and fundamental interest. Using a combination of experimental techniques, Farías *et al.*¹⁹ investigated the propensity for H to migrate into the subsurface of Pd(311), which is a vicinal of Pd(110). Their results point to the dependence of subsurface H diffusion on the coverage and structure of the H overlayer. There is already a debate about the magnitude of the diffusion activation energy barriers for H on Pt(111) and the effect of surface steps on them.²⁰ On Ni surfaces, which are also relevant to studies of hydrogenation, the diffusion barrier for H is found to be in the range of 0.17–0.19 eV.^{21,22} It is thus of interest to examine the corresponding barriers for H diffusion on Pd surfaces.

With the above factors in mind, we used *ab initio* electronic structure calculations for a detailed examination of H adsorption and diffusion on Pd(211) and on Pd(111). The processes studied here are represented schematically in Fig. 1. In the next section, we provide details of the theoretical

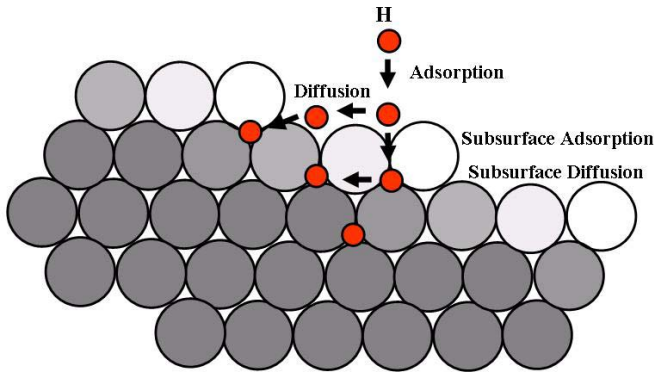


FIG. 1. (Color online) Surface processes studied in this work: surface adsorption, surface diffusion, subsurface adsorption, and subsurface diffusion.

technique that we used. This is followed by Sec. III with a presentation of the results and their discussion, and conclusions are presented in Sec. IV.

II. DETAILS OF THEORETICAL METHODS

Our calculations are based on the density-functional theory,²³ in which the one-particle Kohn-Sham equations are solved self-consistently using a plane-wave basis set in the pseudopotential approach. The exchange and correlation energies are described using the parametrization of Perdew and Wang within the generalized gradient approximation (GGA).²⁴ Ultrasoft pseudopotentials are used for all elements under consideration.²⁵ The cutoff for the kinetic energy of the plane waves is taken to be 200 eV for all calculations. The computer code used was VASP.²⁶ The surface unit cell for H on Pd(111) is taken to be (2×2) (see Fig. 2), i.e., there is one H atom per four Pd atoms, corresponding to a coverage of 0.25 ML (monolayer). For the case of Pd(211), we considered a (2×1) unit cell (see Fig. 3), which also corresponds to a coverage of about 0.25 ML. Note that the (2×2) unit cell of Pd(111) has an area of $5.591 \times 4.841 \text{ \AA}^2$, while the (2×1) unit cell of Pd(211) has a slightly smaller area of $5.591 \times 4.748 \text{ \AA}^2$. Our supercells for Pd(211) and Pd(111) consist of slabs of 15 and 5 Pd layers, respectively. As a result, the total number of Pd atoms for Pd(211) is 30 and that for Pd(111) is 20. In fact, as a result of the differences in the interlayer separations, the 15-layer slab used in the calculations of Pd(211) is just about as thick as the 5-layer one in the calculations of Pd(111). The vacuum space used for Pd(211) and Pd(111) was 16 Å, respectively. Integration over an irreducible Brillouin zone was carried out using the Monkhorst-Pack grid²⁷ of $(12 \times 5 \times 1)$ for Pd(211) and $(6 \times 6 \times 1)$ for Pd(111), which resulted in 12–31 irreducible k points for Pd(211) and 7–20 irreducible k points for Pd(111), depending on the symmetry on the adsorption site. A Fermi-level smearing²⁸ of 0.2 eV was also applied. Hydrogen atoms were placed on the surface sites and their adsorption energy was calculated by allowing all H and Pd atoms to completely relax, except for those in the bottom layers [two layers for Pd(111) and six layers for Pd(211)] which were kept fixed at their positions in the bulk solid.

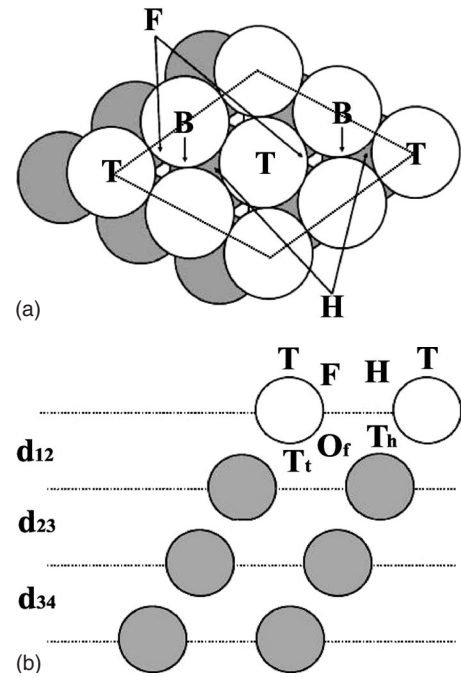


FIG. 2. Possible adsorption sites for H on Pd(111): (a) top view of Pd(111). White and dark circles are Pd atoms in the first and second layers, respectively, while F, H, T, and B represent the fcc and hcp hollow, on-top, and bridge sites, respectively. The (2×2) surface unit cell is marked by the dotted lines. (b) Side view of Pd(111) in which O_f , T_h , and T_t label the octahedral and two tetrahedral subsurface sites, respectively. The d_{ij} 's are the spacings between layers i and j .

Adsorption energy for atomic hydrogen was calculated with respect to hydrogen molecular binding energy in the gas phase using $E_{ad} = E(\text{Pd} + \text{H}) - E(\text{Pd}) - (1/2)E(\text{H}_2)$, where $E(\text{Pd} + \text{H})$ is the calculated total energy of the H/Pd system, $E(\text{Pd})$ is the energy of a similar supercell representing the clean surface, and $E(\text{H}_2)$ is the energy of a H_2 molecule in a cube with dimensions of $10 \times 10 \times 10 \text{ \AA}^3$. These adsorption energies do not include zero-point energy. Our calculated lattice constant for bulk Pd was 3.954 Å, which is 1.6% larger than that of the experimental value of 3.89 Å and is consistent with the general error obtained within DFT-GGA applications to such systems.

III. RESULTS AND DISCUSSIONS

In the following paragraphs, we first discuss the effect of hydrogen adsorption on the multilayer relaxation pattern of Pd(111) and Pd(211). This is followed by presentations of our analysis of H adsorption and diffusion on these two surfaces. For purposes here, we have chosen to examine these characteristics for a set of high symmetry points, which have been the subject of much discussion in the literature. On Pd(111), the sites of interest in the surface layer include that on top of a Pd atom (T), another at the position bridging two Pd atoms (B), and the two hollow sites: fcc (F), which has no atom directly below it in the second layer, and hcp (H) which does have an atom below it (in the second layer). At the

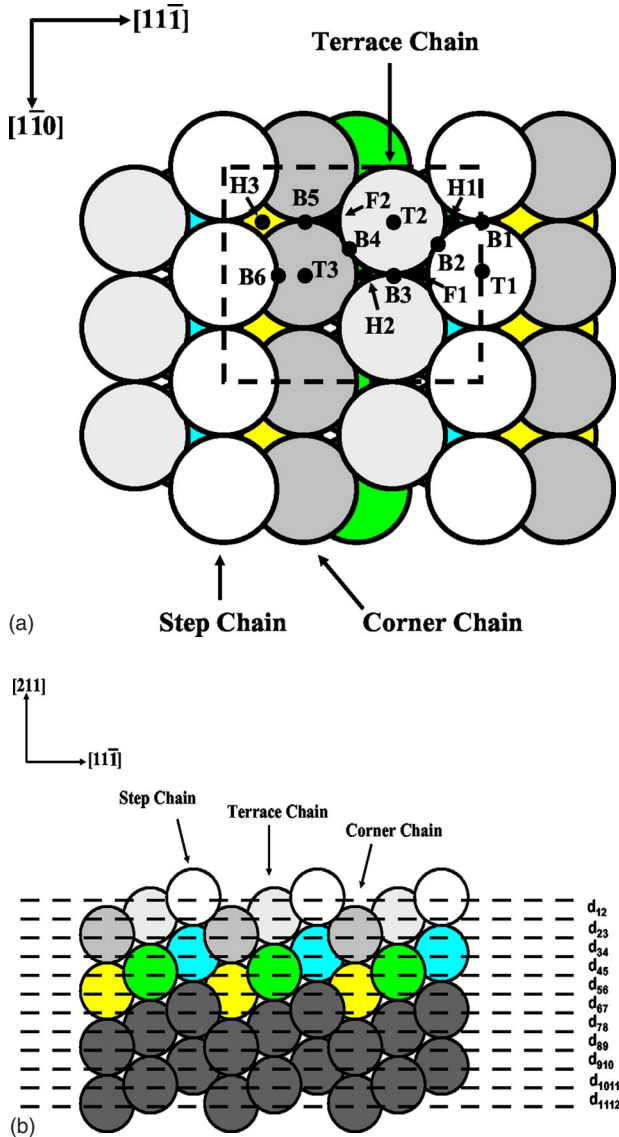


FIG. 3. (Color online) Possible adsorption sites for H on Pd(211). (a) Top view with the (2×1) surface unit cell shown as a dashed rectangle. F, H, T, and B represent the fcc and hcp hollow, on-top, and bridge sites, respectively, except that H3 is the fourfold hollow site on the (100) -faceted step. (b) The side view of Pd(211) showing interlayer separations d_{ij} .

subsurface level, the adsorption sites of concern are the two tetrahedral sites T_t and T_h , which lie below the on-top and hcp hollow sites, respectively, and the octahedral site O_f lying right underneath the fcc hollow site. These sites are shown schematically in Figs. 2(a) and 2(b).

For the vicinal surface Pd(211), as its top view in Fig. 3(a) and side view in Fig. 3(b) indicate, not all on-top, bridge, and hollow sites are equivalent. We have, thus, added another index to our notation for the sites on the terrace to signify the distinction. The (2×1) surface unit cell used in the calculations, shown as a dashed rectangle in Fig. 3(a), thus consists of the sites F_i , H_i , T_i , and B_i representing the fcc and hcp hollow, on-top, and bridge sites, respectively, where i may take values from 1 to 6 to distinguish their local environments. As i increases, the corresponding site is located lower

TABLE I. Calculated structural relaxations of Pd(211) on H surface and subsurface adsorption. Relaxations are given in % of the bulk interlayer distance.

	Clean	F1	H2	O_f1	T_h2
$d_{12}(\%)$	-12.4	-14.4	-21.9	-12.1	-20.0
$d_{23}(\%)$	-13.9	-4.4	-3.7	-4.6	+0.5
$d_{34}(\%)$	+20.1	+14.5	+20.0	+18.2	+15.9
$d_{45}(\%)$	-8.2	-7.6	-12.6	-8.3	+4.9
$d_{56}(\%)$	-1.0	+0.9	+5.0	-0.2	-11.0
$d_{67}(\%)$	+4.0	+3.6	+1.7	+3.9	+4.5
$d_{78}(\%)$	-0.7	-1.1	-1.7	-1.5	-0.1
$d_{89}(\%)$	+0.6	+1.1	+2.3	+1.2	-0.7

in height [refer to Fig. 3(b)] and closer to the corner chain on the left. For example, H2 is located lower and closer to the corner chain on the left than H1, in Fig. 3(a). Note that H3 is a fourfold hollow site on the (100) -faceted step surface. For the subsurface adsorption sites on Pd(211), we use the same labeling scheme as that for Pd(111), i.e., O_h , T_t , and T_h represent the octahedral, and the two tetrahedral subsurface sites, respectively. These subsurface sites also carry corresponding indices (i) to distinguish their local geometry.

A. Effect of H adsorption on multilayer relaxations

For the specific adsorption sites discussed above, we present below our calculated interlayer relaxations. We discuss first the case of Pd(111), followed by that of Pd(211). The results for Pd(211) are summarized in Table I along with other available theoretical and experimental results for comparison. The notations in Figs. 2 and 3 are used in the table.

1. Interlayer relaxation of Pd(111)

Adsorption of H causes the top layer Pd atoms to relax outwards. However, for the coverage considered here (0.25 ML), this relaxation is small: on the average, the spacing between the atoms in the first and second Pd layers changes only by about +1.2%. Note that the four Pd atoms in the surface unit cell are no longer equivalent once the H atom occupies one of the four sites (F, H, B, and T) indicated in Fig. 2(a). H adsorption thus causes a small rumpling of the surface because of the differential outward relaxation of the top layer Pd atoms. More interesting is the case of subsurface H adsorption [sites O_f , T_t , and T_h in Fig. 2(b)], in which the Pd atoms in the vicinity of the adsorbed H atom undergo substantial displacement from their equilibrium positions in clean Pd(111). This pronounced outward expansion of the top layer Pd atoms accompanied by the downward displacement of the Pd atoms in the second layer, which are nearest neighbors of the H atoms, is understandable since room has to be made for the latter. Consider, for instance, adsorption at the tetrahedral site T_t for which the displacement of the Pd atoms is most striking. The separation between the Pd atoms in the first and second layers in the immediate vicinity of the H atom undergoes a shift of about +11% as compared to that

on the clean surface. Here the rumpling of the first layer is undoubtedly remarkable (0.21 Å). For the case of adsorption at O_f and T_h , the corresponding changes in Pd atom spacings are +3% and +5%, respectively. As hydrogen is difficult to detect and easily becomes a surface contaminant like C and S, we wonder if this large relaxation induced by subsurface hydrogen may have been credited with the unusual expansion reported for metal surfaces.^{4,5,29}

Our calculated bond lengths and the height of H above the Pd surface atoms are in general agreement with those reported earlier from theoretical calculations.^{13,15,18} For both hollow sites, we find the height to be 0.81 Å and the H-Pd bond length to be 1.82 Å. These values are in good agreement with experimental results of 0.85 ± 0.05 Å for H height and 1.78 Å for H-Pd bond length.⁹ At the bridge site, we find the height to be 0.98 Å, while the bond length is 1.73 Å. On the other hand, for the least favored adsorption site (on-top), H site at a distance of 1.55 Å. In the case of subsurface adsorption site O_f , the depth of the H atom from its nearest-neighbor top layer is 1.05 Å, while its bond length with the same Pd atom is 1.93 Å. The corresponding depths for T_t and T_h adsorption sites are 1.71 and 0.59 Å, respectively. For the tetrahedral site T_h , the bond length is 1.77 Å.

2. Interlayer relaxation of Pd(211)

The calculated structural relaxations for Pd(211) in the presence of 0.25 ML coverage of H are summarized in Table I. As is already known, there are large interlayer relaxation on the clean Pd(211) surface:^{30,31} Pd atoms in the corner chain [d_{34} in Fig. 3(b)] undergo a large expansion (20% of the bulk interlayer distance), while Pd atoms in the step chain and those in the terrace chain contract by about 12–14% of the bulk interlayer distance, as seen in Table I. As a result, the terrace is not flat any longer, rather it becomes rough and does not possess the ideal surface registry of Pd(111). We find that the adsorption of hydrogen on the Pd(211) terrace produces H-Pd bond lengths (1.83 Å for H2 and 1.82 Å for F1) similar to that on Pd(111). H adsorption at the H2 site also displays a larger contraction (22%) for d_{12} as compared to that for the clean surface, while that at site F1 (14%) produces about the same change in d_{12} as that for the clean surface. As indicated by the entries in Table I, the contraction of d_{23} is remarkably small for on-surface H adsorption, showing values of about 4% as compared to 14% on the clean surface. These changes in the bond lengths are the result of the outward relaxation of the second layer (the Pd atoms in the terrace chain) upon H adsorption in the terrace.

For the subsurface sites in Pd(211), as in the case of Pd(111), H adsorption in O_f (directly below F1) does not show a substantial change in relaxation, from clean surface value, while that in T_h 2 (directly below H2) results in a large expansion of the second layer, which causes the change in d_{23} to become positive (+0.5%), instead of the negative values found for all the other cases of d_{23} in Table I. A very pronounced relaxation, similar to that exhibited by Pd(211), is predicted for clean Pd(210): -17%, -3%, and +10% for the first, second, and third layers, respectively.⁴ For Pd(210), however, a much smaller contraction (-3%) for the first

layer and a large expansion (+7%) for the second layer were observed, and these were attributed to residual hydrogen coverage of less than 0.25 ML.²⁹ Our results show that when H adsorbs on the terrace, the contraction of d_{23} (from bulk values) is markedly reduced by about 10% [from -14% for Pd(211) to about -4% for H-covered Pd(211)]. Moreover, when H adsorbs at T_h 2 in the subsurface, this reduction could be about 14%, i.e., d_{23} reverts to the bulk value. Thus, residual hydrogen and, in particular, subsurface hydrogen can make a significant difference in interlayer separations observed experimentally and need to be carefully taken into account in the analysis of such data.

B. Energetics of H adsorption

In this section, we summarize the results of our calculations of E_{ad} , the adsorption energy, for H on Pd(211). For reference, we have also calculated E_{ad} for various sites on the mother surface Pd(111), for which we provide a comparison of our results with those available in the literature. We present first the results for Pd(111).

1. Adsorption energy of a submonolayer of H on Pd(111)

For the seven possible sites labeled in Fig. 2, we present in Table II our calculated adsorption energies for 0.25 ML hydrogen on Pd(111). The hollow sites of Pd(111) display the largest adsorption energy, the fcc site with E_{ad} of -0.59 eV is slightly preferred over the hcp one (by 0.04 eV), in agreement with previous calculations.^{14,16} Note that Ref. 18 predicted the converse to be the case. The bridge site with E_{ad} of -0.44 eV offers somewhat lower adsorption energy while the on-top site is out of consideration, its adsorption energy being just -0.05 eV. In summary, our results exhibit a trend that H prefers a highly coordinated site for adsorption on Pd(111). More importantly, adsorption energies for the octahedral and tetrahedral subsurface sites are much smaller than those for on-surface adsorption. Among the subsurface sites, the octahedral with E_{ad} of -0.23 eV has the larger adsorption energy, followed closely by those at the two tetrahedral sites. These results naturally favor on-surface adsorption over the subsurface one by more than 0.36 eV, at 0.25 ML coverage, in agreement with previous theoretical calculations,^{13–18} the results of which are also summarized in Table II. We point out that our calculated value for the most preferred site is not in perfect agreement with the experimental E_{ad} reported in Ref. 1. For the same coverage, Løvvik and Olsen¹⁶ found good agreement with experiment for E_{ad} for adsorption in the hollow site. Since our results also show preference for the hollow sites, our calculated E_{ad} is larger than that found experimentally, but lies within the range of values found theoretically. This overestimation of E_{ad} in calculations based on DFT-GGA is a subject of investigation which we defer to the future.

2. Adsorption energy of a submonolayer of H on Pd(211)

The roughness of the clean Pd(211) surface, as a result of the differential interlayer relaxation discussed above, is expected to induce substantial variations in the site-specific adsorption energetics for this stepped surface since the local

TABLE II. Calculated values of E_{ad} (in eV) for H adsorption on Pd(111). The surface sites F, H, T, and B and the subsurface sites O_f , T_t , and T_h are as indicated in Fig. 2.

	Coverage (ML)	F	H	T	B	T_t	T_h	O_f
This study	0.25	-0.59	-0.55	-0.05	-0.44	-0.19	-0.20	-0.23
Watson <i>et al.</i> ^a	0.25	-0.50	-0.44	+0.01	-0.35			
Dong and Hafner ^b	0.25	-0.69	-0.65	-0.01	-0.41			
Paul and Sautet ^c	0.33	-0.54						-0.42
Løvrvik and Olsen ^d	0.25	-0.44	-0.41	-0.32				
	0.33	-0.54	-0.47	-0.12	-0.39			+0.02
Löber and Henning ^e	0.33	-0.37	-0.43					-0.23
Expt. ^f				-0.45				

^aReference 13.

^bReference 14.

^cReference 15.

^dReference 16.

^eReference 18.

^fReference 1.

geometry experienced by hydrogen is not the same as that on flat Pd(111). These changes are made apparent in the summary of the adsorption energy for H on Pd(211) presented in Table III. Basically, a trend similar to the Pd(111) surface is repeated, i.e., the threefold hollow sites (F1-F2 and H1-H2) are preferred although the entries in Table III suggest that some of the bridge and on-top sites are not to be excluded. However, there are a couple of interesting changes. First, for adsorption in the threefold hollow sites, there is very little difference in the energy between the fcc and hcp sites. The hcp hollow site labeled H2 (Fig. 3) is the preferred adsorption site with energy of -0.52 eV, which is close to E_{ad} on Pd(111) (-0.55 eV). This may be attributed to the fact that H2 is located on the terrace where its local geometry is closest to that on Pd(111). In general, in a one-to-one comparison of adsorption sites, we find smaller adsorption energies on the (211) surface than those on the (111) surface. Such a reduction of the adsorption energy was also observed for Pd(210): E_{ad} on Pd(100) was found to be 0.53 eV,³² but on Pd(210) it was 0.41 eV.^{4,33} The lowering of adsorption energy may also be accompanied by a lowering of the diffusion barriers and may reflect an increase of reactivity of the stepped surface. Second, the fourfold hollow site (H3), with adsorption energy 0.43 eV, is energetically less favored than the threefold hollow sites. Third, the on-top site adsorption, T3, is understandably equivalent to the twofold bridge site (B6) in Fig. 3(a): at T3 the hydrogen atom is right above the Pd atoms in the corner chain along the surface normal and

easily falls onto the bridge site (B6). Last, for subsurface adsorption, the difference in energy between the octahedral (O_f) and the tetrahedral (T_h) sites is much smaller for Pd(211) than it is for Pd(111).

A plot of the adsorption energy versus the local coordination of the H atom, in Fig. 4, shows that hydrogen generally prefers a high coordination site on Pd(211). The one exception is adsorption in the “fourfold” hollow site (H3), which is a special case since it is at the step edge and not on the terrace. It is interesting to note that on Pd(210), the ordering of the adsorption sites with adsorption strength correlated the geometrical average of the nearest-neighbor *d*-band centers.⁴ We carried out calculations of the *d*-band centers of the Pd atoms on Pd(211) that are nearest neighbor of the adsorbed H and did not find any such correlation. H adsorption at site H3 deserves special attention on another note. In the case of the adsorption of C or S on Pd(211), this fourfold hollow site at the step edge was the most preferred site,^{30,31} and in the case of C, it even penetrated the (100)-faceted plane so that it made an additional bond with the Pd atom in the fourth layer. For the much smaller atom, hydrogen, it is natural to expect

TABLE III. Same as in Table II but for Pd(211). The site labels and indices are the same as in Fig. 3.

Site index	F	H	T	B	T_t	T_h	O_f
1	-0.516	-0.508	+0.03	-0.438	-0.134	-0.183	-0.193
2	-0.518	-0.522	-0.03	-0.386		-0.162	
3		-0.428	-0.389	-0.415	-0.133		
4				-0.414			
5				-0.362			

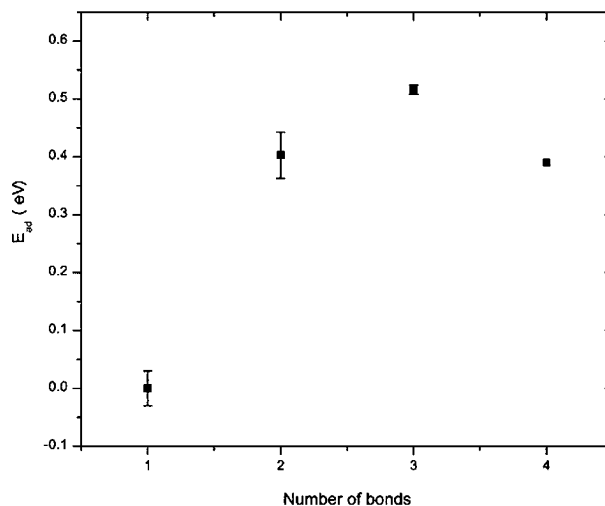
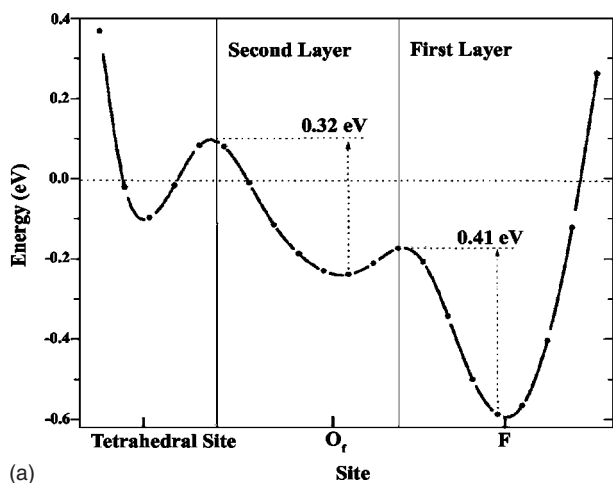
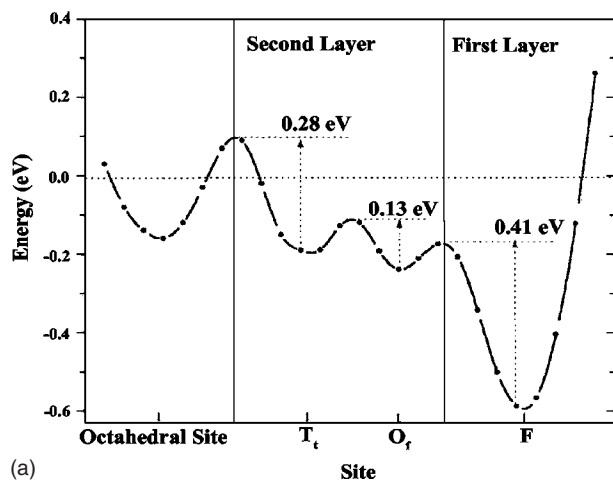


FIG. 4. Correlation between the H adsorption energy and the coordination of the adsorption sites in Fig. 3.



(a)



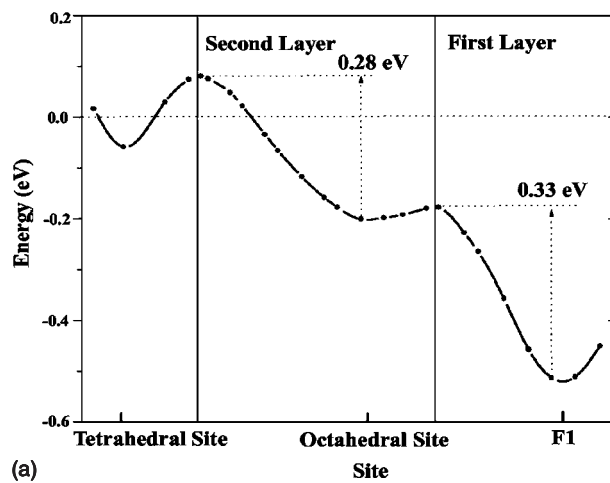
(a)

FIG. 5. The calculated energy profile of H surface to subsurface diffusion at Pd(111). Results are plotted for (a) the straight path through the fcc hollow site at the surface and the octahedral site in the subsurface; (b) for a path similar to (a), but including the octahedral and tetrahedral sites in the subsurface region, and the octahedral site below the second layer. Reference energy is $E[\text{Pd}(111)] + (1/2)E[\text{H}_2]$.

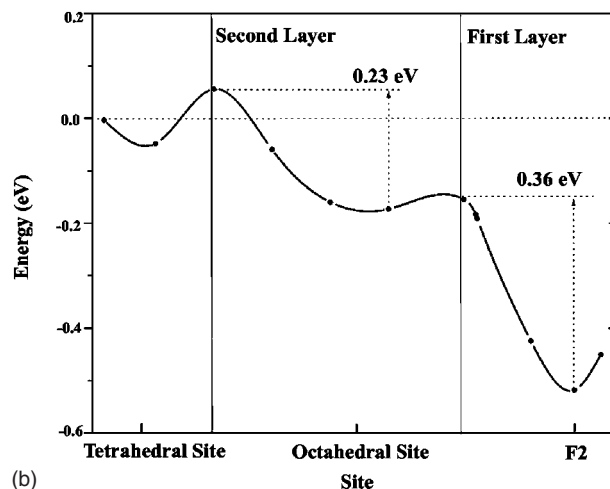
a behavior similar to that for C, but this turns out not to be the case. We found that even if the hydrogen atom is manually pushed into the (100)-faceted plane, it immediately pops out of the plane. Clearly the changes in the electronic structure of Pd(211) induced by C are not the same as that done by H.

C. Energy landscape for H diffusion from surface to subsurface on Pd(111) and Pd(211)

Our calculated energy profile of H for Pd(111) and Pd(211) along two chosen paths from the surface to the subsurface regions are shown in Figs. 5 and 6, respectively. For each point in the calculation, the submonolayer of hydrogen is placed in the specific configuration on the surface, in the subsurface region, and in the bulklike region, step by step along a given path. The total energy of the configuration is calculated according to the prescription provided in Sec. II, except that the H atom is allowed to relax in the direction



(a)



(b)

FIG. 6. The calculated energy profile of H surface to subsurface diffusion at Pd(211). Results are plotted for straight paths through (a) F1 at surface and O_{f1} in the subsurface, and (b) F2 at surface and O_{f2} in the subsurface. Reference energy is $E[\text{Pd}(211)] + (1/2)E[\text{H}_2]$.

normal to the path but not along the path. From the calculated energy profile, we estimated the energy barrier for H diffusion along these paths. We realized that more definitive calculations of the energy barrier required calculation of the exact transition state for the process (saddle point) in a multidimensional phase space. The intent here, however, was to examine the relative trends in the probability of H diffusion along chosen paths. In Fig. 5(a), the total energy difference with respect to that for $\text{Pd}(111) + (1/2)\text{H}_2$ system is plotted for a large number of points (about 25) along the path from site F [Fig. 2(b)] into the third layer atoms directly below it. Clearly the hydrogen atom prefers to stay at F and needs 0.41 eV to go into the subsurface region and, from subsurface to the bulk region, another 0.32 eV is needed. In Fig. 5(b), we plotted the same energy difference, but for another path originating from F. Here we examined the energy landscape for H as it tries to sample the region from O_f to T_t and then straight down into the third layer. On comparing Figs. 5(a) and 5(b), we saw that the propensity for H to go into the bulk via the tetrahedral site T_t is larger than going straight down from the octahedral site O_f .

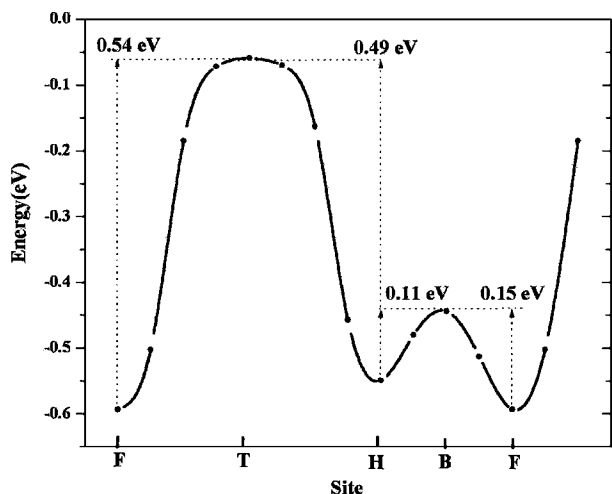


FIG. 7. The calculated energy profile of H surface diffusion on Pd(111). Results are plotted for path connecting F–B–H–T–F. The reference energy is $E[\text{Pd}(111)] + (1/2)E[\text{H}_2]$.

The energy profile for H along two paths from points on the surface of Pd(211) into its bulk are presented in Figs. 6(a) and 6(b). In Fig. 6(a), we started with the H at the threefold fcc hollow site F1 [see Fig. 3(a)] and proceeded straight down into the bulk along a path normal to the terrace. As seen, H is in equilibrium at the site F1 and requires about 0.33 eV to move to the octahedral site O_f1 , from where it needs another 0.28 eV to get to the tetrahedral site beneath the second layer. If, on the other hand, H is in equilibrium at the site F2 near the step edge, it needs 0.36 eV to overcome the barrier to reach the octahedral site O_f2 and a subsequent energy of 0.23 eV to get to the tetrahedral site below the second layer.

On comparing the energetics for H penetration from the surface to the subsurface on Pd(211) and Pd(111), we found that the initial difference of 0.08 eV in the barriers between the surface fcc hollow site and subsurface octahedral site 0.41 eV for Pd(111) and 0.33 eV for Pd(211) is the main basis for arguing that the stepped surface may be more susceptible for subsurface H presence than the flat one, and the reduction comes from the decrease of the adsorption energy of hydrogen in the hollow sites of Pd(211) as discussed earlier. The energy barrier for H to move from the subsurface to the bulk region for Pd(211) is slightly larger (by about 0.04 eV) than that for Pd(111). From Figs. 5 and 6, it is evident that only after the hollow sites on surface are substantially populated, hydrogen will start to dissolve into the bulk;^{1,19} otherwise, H will immediately diffuse back to the surface. This also applies for the diffusion from subsurface to the bulk regions. When the surface is empty and temperature is high enough for the absorbed H atoms in the bulk region to overcome the barrier, they will diffuse back into the surface and populate the surface again. As a result, surface hydrogen comes from two sources: one from the region above the surface, and the other is the absorbed hydrogen traveling back through the bulk region, as observed in thermal desorption spectroscopy (TDS) experiment.¹

While our results may be in apparent conflict with the experimental finding that at even low temperatures the sub-

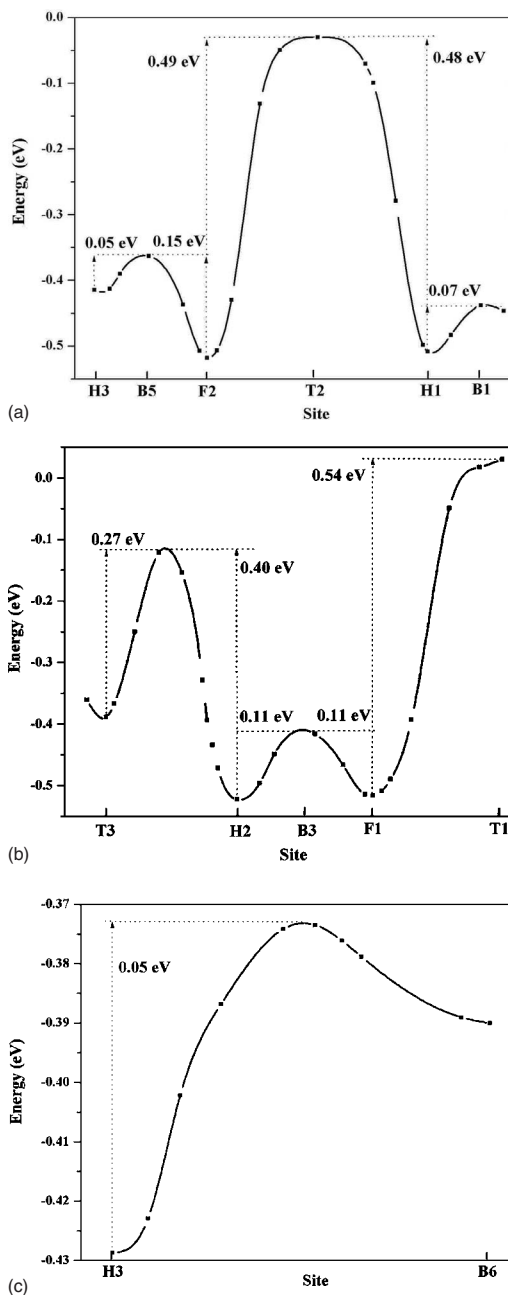


FIG. 8. The calculated energy profile of H surface diffusion on Pd(211). Results are plotted for paths connecting: (a) B1–H1–T2–F2–B5–H3, (b) T1–F1–B3–H2–T3, and (c) H3–B6 along the step chain. The reference energy is $E[\text{Pd}(211)] + (1/2)E[\text{H}_2]$.

surface site was populated, there are some important factors that should be taken into account. First, there may be concerted H absorption and adsorption. According to Löber and Hennig¹⁸ while the energy barrier for H diffusion from a surface to a subsurface site on a hydrogen preadsorbed Pd(111) surface is 0.74 eV, it reduces to 0.43 eV in the case of simultaneous H adsorption and subsurface diffusion. Second, there may be a coupling of H subsurface adsorption to a surface phonon. That is, a highly coordinated motion of H and the surface Pd atoms may drastically reduce the subsurface energy barrier, as predicted by Løvrvik and Olsen.¹⁶ In fact, the energy barrier was found to disappear altogether.

Third, there may be a strong dependence of the subsurface adsorption barrier on H coverage. For example, for subsurface adsorption of 1 ML hydrogen, the barrier was calculated to be 0.85 eV.¹⁶ This value reduces to 0.74 eV for 2/3 ML,¹⁶ and in our study, it reduces further to 0.33 eV for 0.25 ML hydrogen. This trend of decreasing energy barrier with decreasing coverage appears to suggest the possibility of subsurface adsorption at very small coverages. Recent calculations by Nobuhara *et al.*,³⁴ however, effectively showed no change in this energy barrier as the coverage is reduced from 1/4 ML to 1/9 ML. Fourth, there may be quantum-mechanical effects such as tunneling responsible for H penetration into the surface. Low-temperature hydrogen diffusion often shows crossover from classical overbarrier hopping to quantum-mechanical underbarrier tunneling.²¹ For example, for H diffusion on Ni(111), a crossover was observed to occur at 110 K with a reduced activation energy of about 0.1 eV.²¹ On Pd(111), experiments suggesting hydrogen occupation of a subsurface site were carried out at temperatures as low as 80 K.⁵⁻⁹ It is reasonable to assume that at this temperature H penetration from Pd(111) surface to subsurface may occur via underbarrier tunneling rather than overbarrier hopping. It may also require less energy barrier. Thus to get a full agreement with experimental data, one has to perform a coverage, temperature, and pressure dependent quantum-mechanical calculation of the adsorption rate. Such a calculation is beyond the scope of this work.

D. Energy landscape for H surface diffusion on Pd(211) and Pd(111)

The calculated energy profile for H at chosen points along the paths connecting the four adsorption sites (F, H, T, and B) on Pd(111) is illustrated in Fig. 7. As expected from the results in Sec. III B above, there is an activation energy barrier of about 0.54 eV for H to jump from the fcc hollow site to the on-top position from where it can easily go to the hcp hollow site. The activation energy barrier from the hcp to the fcc hollow site, via the bridge site, is only 0.11 eV. From the most preferred adsorption site (F), the activation energy barrier is 0.15 eV, which may be taken as the representative energy barrier for H diffusion on Pd(111). This latter value is comparable to that deduced from experiments for H on Pt(111), which report these energy barriers to be 0.07,³⁵ 0.16,²⁰ and 0.19 eV.³⁶ These differences in the values arise from the subtleties in the experimental techniques and continue to be the subject of discussion.²⁰ Regardless, it is satisfying to see that our calculated energy barrier for H on Pd(111) lies in the range found in experiments, albeit on Pt(111).

Next we turn to the calculated energy landscape for H on Pd(211) along three chosen paths: (1) away from the step edge from H3 to B1, (2) away from the step edge from site T3 to T1, and (3) along the step edge from site H3 to B6 [see Fig. 3(a)]. Although a number of other diffusion paths are conceivable on this stepped surface, the three chosen above provide the maximum and minimum energy barriers faced by the H atoms as they try to diffuse on the terraces of Pd(211), which consist of three inequivalent hcp sites, two inequiva-

lent fcc sites, six inequivalent bridge sites, etc. From the site-specific adsorption energies presented in Table III and the information below, the activation energy barrier for any path on Pd(211) can be obtained.

The calculated energy profile for H along path 1 (H3 to B1) on Pd(211) is presented in Fig. 8(a). Along this path, the lowest energy point is at F2. H atom adsorbing near the step edge at H3 needs only 0.05 eV to overcome the barrier at the bridge site (B5) and reach the hollow site F2, beyond which it has to surmount a barrier of 0.49 eV to get to the on-top site T2 before settling into the hollow site H1 near the next step edge. Conversely, H adsorbed at F2 needs to overcome a barrier of 0.15 eV to reach the step edge.

The diffusion energy barriers for the H atom initially adsorbed near the step edge at T3 follow a different structure from the one above, for our chosen path 2, as depicted in Fig. 8(b). It needs to first overcome a barrier of 0.27 eV to reach H2, which according to Table III is the most favored. From H2, the energy barrier to the next hollow fcc site is 0.11 eV, as found earlier on Pd(111). This is not surprising since the terraces of Pd(211) have the same geometry as Pd(111). There is, however, a difference in the characteristics of H diffusion on the two surfaces. As we have shown in Table III, there are several adsorption sites for H on Pd(211) with small differences in adsorption energy. Also H would most likely adsorb on one of the sites near the step edge (higher adsorption energy). From these sites, H could diffuse to the other sites through the paths with energy barriers of about 0.11 eV (see Table III), which is 0.04 eV less than the typical diffusion barrier that it finds on Pd(111).

The most pronounced evidence for H diffusion on Pd(211) comes from the plot in Fig. 8(c) of its energy profile along the step edge (path 3). Here the activation energy barrier from H3 to B6 is only 0.05 eV—three times lower than that found for Pd(111). These results also point to an enhanced H diffusion *along* the step edge rather than *away* from it. This shows that the diffusion path along the step edge is like a nanoscale highway where hydrogen atoms can diffuse very fast from one place to another on Pd(211). Also, the existence of such a fast diffusion path may suggest that the step is a very reactive place for Pd(211).

E. Energy landscape for subsurface H diffusion on Pd(211) and Pd(111)

Although the subsurface sites on Pd(111) have lower adsorption energy than the hollow and bridge sites in the surface layer, the probability for finding H in the subsurface region is not negligible. In Fig. 9, we plotted the energy profile for H as it attempts to diffuse from the octahedral site to the tetrahedral ones. The diffusion energy barrier is about 0.12 eV, except for the jump between the tetrahedral sites T_h and T_t , for which the barrier is 0.23 eV. Thus from considerations of energetics alone, once H penetrates into the subsurface region, it can diffuse with somewhat greater ease than on Pd(111) surface.

On Pd(211), we have calculated the energy profile for H in the subsurface region only along a path directly below path 2, considered above in Sec. III D as specific example.

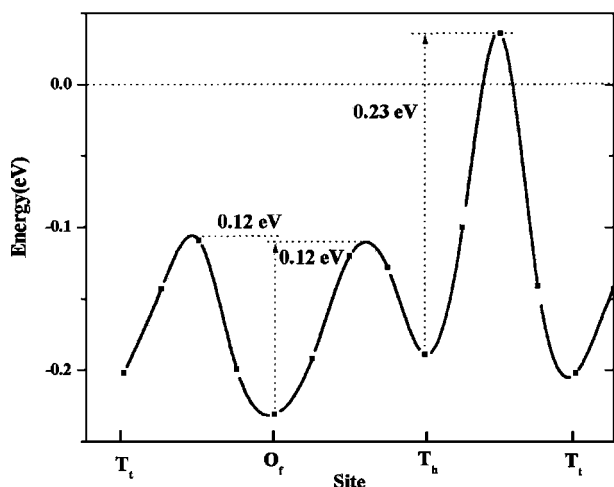


FIG. 9. The calculated energy profile of H subsurface diffusion in Pd(111). Results are plotted for path connecting T_t-O_f-T_h-T_t. The reference energy is $E[\text{Pd}(111)] + (1/2)E[\text{H}_2]$.

The plot in Fig. 10 shows the activation energy barrier to vary from 0.06 to 0.31 eV. The typical activation energy barrier for the subsurface diffusion on Pd(111) and Pd(211) is an order of 0.1 eV, and this small barrier can be easily exploited for manipulation of a subsurface H atom by exciting it with the electric current or the electromagnetic wave. For example, in Ref. 5, the subsurface H atoms were freely moved by exciting it with the electric current using a scanning tunneling microscope tip.

To examine the possibility of H to penetrate into the bulk on Pd(211) through adsorption near the step edge, we present in Fig. 11 our calculated the energy profile for H diffusion from the surface site H3 to the subsurface T_h1 through the (100)-faceted step. The energy barrier from Fig. 11 is 0.38 eV. The transition point (the potential peak) of the graph does not lie right on the step plane, but slightly inside the plane, as discussed earlier. Thus, H does not automati-

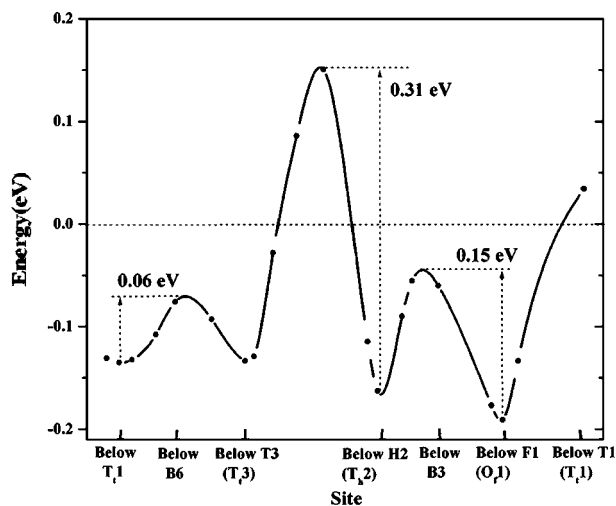


FIG. 10. The calculated energy profile of H surface to subsurface diffusion in Pd(211). Results are plotted for path connecting the points below F1, H2, T3, and T₁1. The reference energy is $E[\text{Pd}(211)] + (1/2)E[\text{H}_2]$.

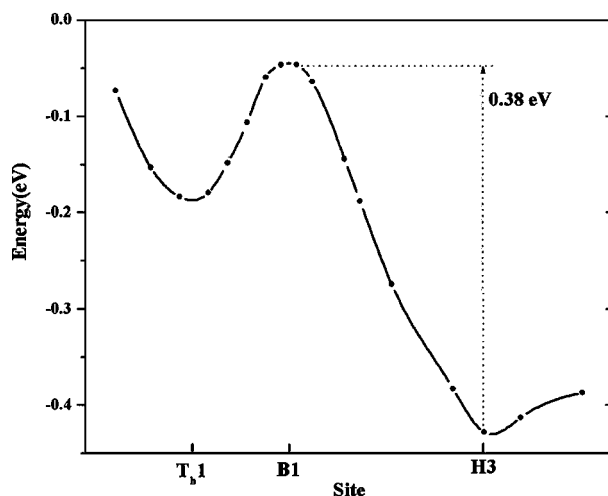


FIG. 11. The calculated energy profile of H surface-to-subsurface diffusion through the step for Pd(211). Results are plotted for the path: H3-B1-T_h1. The reference energy is $E[\text{Pd}(211)] + (1/2)E[\text{H}_2]$.

cally penetrate the rather open (100) plane like a C atom. Therefore, it is not the size of an atom but the interaction of an atom with the Pd atoms both at the surface and in the subsurface site that determines the energy barrier for the subsurface adsorption.

IV. CONCLUSIONS

We performed first-principles calculations of H adsorption and diffusion on Pd(211) using density-functional theory with the generalized gradient approximation in the plane-wave basis. Our calculations showed a number of adsorption sites for H on the Pd(211) terrace and near the step edge for which the adsorption energy lies in the range from -0.52 to -0.4 eV. For H subsurface adsorption, the octahedral subsurface site (directly below the fcc hollow site) is slightly more favorable than the tetrahedral site (directly below the hcp hollow site), with the adsorption energy of 0.19 eV. Our calculated activation energy of H diffusion from the surface to the subsurface is 0.33 eV [0.41 eV for Pd(111) surface]. Thus, an enhancement of hydrogen subsurface adsorption may be expected for Pd(211) as compared to that on Pd(111). A similar order of mobility was also obtained for hydrogen diffusion in the surface and subsurface regions of Pd(211). In particular, we found that the diffusion barrier associated with motion parallel to the step edge is only 0.05 eV on Pd(211). We traced these differential energetics for H on Pd(211) to the differences in the local geometry and changes induced in the interlayer spacings on H adsorption. Our calculations also showed that all subsurface sites are energetically less favorable than the adsorption site on the surface for H. The calculated diffusion barriers and energy profiles for H on Pd(211) and Pd(111) in the surface, subsurface, and from surface to subsurface, however, cannot rule out that a small number of H may penetrate the surface any time. We await more experimental data on H diffusion on the system to establish the validity of the results presented here.

ACKNOWLEDGMENTS

This work was supported in part by grants from DOE (DE-FG02-03ER15842) and NSF (CHE-0548632). Computational resources were provided by NSF Cyberinfrastructure

and TeraGrid Grant No. DMR060035N. T.S.R. also acknowledges the support of the Alexander von Humboldt Foundation and thanks her colleagues at the Fritz Haber Institut, Berlin, for their warm hospitality. We are grateful to Guenther Rupprechter for helpful discussions.

-
- *Corresponding author. FAX: 407 823 5112. Electronic address: talat@physics.ucf.edu. Homepage: <http://www.physics.ucf.edu/~talat>
- ¹H. Conrad, G. Ertl, and E. E. Latta, *Surf. Sci.* **41**, 435 (1974).
 - ²T. Engel and H. Kuipers, *Surf. Sci.* **90**, 162 (1979).
 - ³M. Lischka and A. Groß, *Hydrogen on Palladium: A Model System for the Interaction of Atoms and Molecules with Metal Surfaces*, Recent Developments in Vacuum Science and Technology, edited by J. Dabrowski (Research Signpost, Kerala, 2003), pp. 111–132.
 - ⁴M. Lischka and A. Groß, *Phys. Rev. B* **65**, 075420 (2002); P. K. Schmidt, K. Christmann, G. Kresse, J. Hafner, M. Lischka, and A. Groß, *Phys. Rev. Lett.* **87**, 096103 (2001).
 - ⁵E. C. H. Sykes, L. C. Fernández-Torres, S. U. Nanayakkara, B. A. Mantooth, R. M. Nevin, and P. S. Weiss, *Proc. Natl. Acad. Sci. U.S.A.* **102**, 17907 (2005).
 - ⁶W. Eberhardt, F. Greuter, and E. W. Plummer, *Phys. Rev. Lett.* **46**, 1085 (1981); W. Eberhardt, S. G. Louie, and E. W. Plummer, *Phys. Rev. B* **28**, 465 (1983).
 - ⁷G. E. Gdowski, T. E. Felter, and R. H. Stulen, *Surf. Sci. Lett.* **181**, L147 (1987); G. E. Gdowski, R. H. Stulen, and T. E. Felter, *J. Vac. Sci. Technol. A* **5**, 1103 (1987).
 - ⁸G. D. Kubiak and R. H. Stulen, *J. Vac. Sci. Technol. A* **4**, 1427 (1986).
 - ⁹T. E. Felter, E. C. Sowa, and M. A. Van Hove, *Phys. Rev. B* **40**, 891 (1989).
 - ¹⁰M. S. Daw and S. M. Foiles, *Phys. Rev. B* **35**, 2128 (1987).
 - ¹¹T. E. Felter, S. M. Foiles, M. S. Daw, and R. H. Stulen, *Surf. Sci. Lett.* **171**, L379 (1986).
 - ¹²S. W. Rick, D. L. Lynch, and J. D. Doll, *J. Chem. Phys.* **99**, 8183 (1993).
 - ¹³G. W. Watson, R. P. K. Wells, D. J. Willock, and G. J. Hutchings, *J. Phys. Chem. B* **105**, 4889 (2001).
 - ¹⁴W. Dong and J. Hafner, *Phys. Rev. B* **56**, 15396 (1997).
 - ¹⁵J.-F. Paul and P. Sautet, *Phys. Rev. B* **53**, 8015 (1996).
 - ¹⁶O. M. Løvvik and R. A. Olsen, *Phys. Rev. B* **58**, 10890 (1998).
 - ¹⁷W. Dong, V. Ledentu, P. Sautet, A. Eichler, and J. Hafner, *Surf. Sci.* **411**, 123 (1998).
 - ¹⁸R. Löber and D. Hennig, *Phys. Rev. B* **55**, 4761 (1997).
 - ¹⁹Farías, P. Schilbe, M. Patting, and K.-H. Rieder, *J. Chem. Phys.* **110**, 559 (1999).
 - ²⁰C. Z. Zheng, C. K. Yeung, M. M. T. Loy, and X. Xiao, *Phys. Rev. B* **70**, 205402 (2004); *Phys. Rev. Lett.* **97**, 166101 (2006).
 - ²¹G. X. Cao, E. Nabighian, and X. D. Zhu, *Phys. Rev. Lett.* **79**, 3696 (1997).
 - ²²T.-S. Lin and R. Gomer, *Surf. Sci.* **225**, 41 (1991).
 - ²³W. Kohn and L. J. Sham, *Phys. Rev.* **140**, A1133 (1965).
 - ²⁴J. P. Perdew and Y. Wang, *Phys. Rev. B* **45**, 13244 (1992).
 - ²⁵D. Vanderbilt, *Phys. Rev. B* **41**, 7892 (1990).
 - ²⁶G. Kresse and J. Hafner, *Phys. Rev. B* **47**, 558 (1993); **49**, 14251 (1994); G. Kresse and J. Furthmüller, *Comput. Mater. Sci.* **6**, 15 (1996); *Phys. Rev. B* **54**, 11169 (1996).
 - ²⁷H. J. Monkhorst and J. D. Pack, *Phys. Rev. B* **13**, 5188 (1976).
 - ²⁸M. Methfessel and A. Paxton, *Phys. Rev. B* **40**, 3616 (1989).
 - ²⁹D. Kolthoff, H. Pfnür, A. G. Fedorus, V. Koval, and A. G. Naumovets, *Surf. Sci.* **439**, 224 (1999).
 - ³⁰S. Stolbov, F. Mehmood, T. S. Rahman, M. Alatalo, I. Makkonen, and P. Salo, *Phys. Rev. B* **70**, 155410 (2004).
 - ³¹I. Makkonen, P. Salo, M. Alatalo, and T. S. Rahman, *Phys. Rev. B* **67**, 165415 (2003).
 - ³²R. J. Behm, K. Christmann, and G. Ertl, *Surf. Sci.* **99**, 320 (1980).
 - ³³U. Muschiol, P. K. Schmidt, and K. Christmann, *Surf. Sci.* **395**, 182 (1998).
 - ³⁴K. Nobuhara, H. Kasai, H. Nakanishi, and A. Okiji, *J. Appl. Phys.* **92**, 5704 (2002).
 - ³⁵A. P. Graham, A. Menzel, and J. P. Toennies, *J. Chem. Phys.* **111**, 1676 (1999).
 - ³⁶R. Lewis and R. Gomer, *Surf. Sci.* **17**, 333 (1969).